Article

A Lateral Control Method of Intelligent Vehicles Based on Shared Control

Gang Li , **Pengfei Shang, Changbing Zheng and Dehui Sun** *

Key Laboratory of Field Bus Technology and Automation of Beijing, North China University of Technology, Beijing 100144, China
* Correspondence: sundehui@ncut.edu.cn

Abstract: This paper studies the lateral control problem for intelligent vehicles based on the concept of shared control. Considering the participation of drivers in the control loop, a shared control-based lateral controller is designed, which consists of two differed controllers: one is an LQR-based autonomous driving controller and the other is a driver's intention-based fuzzy controller. For the vehicle dynamic model with two-degrees of freedom, an autonomous driving controller based on LQR and a driver's intention-based fuzzy controller are designed. Then, the lateral controller based on shared control is constructed, which integrates the aforementioned two controllers. Finally, the co-simulation by MATLAB/Simulink and Carsim is presented. Furthermore, simulation results show that the designed lateral controller can track the desired path with better performance than the LQR-based autonomous driving controller.

Keywords: intelligent vehicles; lateral control; shared control

1. Introduction

In recent years, with the rapid development of new techniques such as 5G, big data, cloud computing and AI, the intelligence of the automotive industry and the traditional cars are gradually developing into intelligent vehicles [1–4]. Since intelligent vehicles have great potential to improve road safety, passenger comfort, energy conservation, and emission reduction [5], they have become research hotspots. Furthermore, remarkable results have been achieved [6]. Network advanced communication techniques support the connectivity of intelligent vehicles despite their reduced perception ability, which improve the environmental perception of self-driving cars [7–9].

To measure the level of autonomous driving, the Society of Automotive Engineers International has released a classification system based on the level of driver intervention and attention, these include levels of autonomy for self-driving cars ranging from L0 to L5, and research on self-driving cars is generally focused on L3 level [10]. Currently, the intelligent vehicles with partial or fully autonomous driving functions are becoming increasingly mature, and have been used in unmanned shuttle, courier delivery and unmanned ferry. Many cities allow autonomous vehicles to test and operate. For example, the Toyota e-Palette self-driving minibus served as a ferry for athletes in the Olympic Village during the Tokyo Olympic and Paralympic Games; Baidu Apollo self-driving cars and driverless micro-circulation buses have been operating for a long time in the Shougang Park, the office of the Beijing Winter Olympic Organizing Committee. As pointed out in [11], autonomous vehicles were permissible in several states in the United States, even without the necessity of drivers.

However, the self-driving still faces challenges. Although Waymo announced plans in March 2022 to remove safety drivers for fully autonomous rides in [12], only a few intelligent transportation systems in specific scenarios can achieve a high-level autonomy in the actual traffic environment. In addition, the sensing networks deployed by intelligent vehicles cannot cover complex traffic environments. As stated in the White Book on Traffic Safety of Self-Driving Cars released by CAC and Baidu, the road testing permits were

issued by the California Department of Motor Vehicles in April 2014. The statistical results showed that 149 accidents occurred in real road testing of self-driving cars and 105 accidents occurred during driver takeover between 2019 and mid-2020. Especially, an e-Palette self-driving bus struck and injured a blind athlete while turning right into a crosswalk during the Tokyo Paralympic Games. Consequently, the self-driving bus was taken out of service.

The above description illustrates that there are still many issues to be resolved to achieve a breakthrough in high-level autonomous driving technique without human involvement. As is known to all, it is not only limited by the technological development, but also by the constraints of relevant legal imperfections. At present, most autonomous vehicles still need the participation of drivers, which provides guidance and assess the potential hazards in the presence of the failed algorithm. The human–machine cooperative control uses the asymmetric advantages of human intelligence and machine intelligence, for achieving the hybrid enhancement of human–machine intelligence and the two-way information exchange. Therefore, the active safety assisted control or shared control technology with human involvement is expected to reduce traffic accidents [13]. Notely, the human–machine shared control method has been widely used in auxiliary robots [14,15], remote operation robots [16,17] and intelligent vehicles [18], which balances the advantages of driver and automatic vehicles to achieve the best cooperation [19–21]. Shared control provides a solution to the problem for driving controller conversion of intelligent vehicles [22].

Therefore, this paper designs a shared control-based method to achieve the lateral motion control of intelligent vehicles with driver's participation. The main contributions of this paper are summarized as follows.

1. To achieve the flexible shared control, a model-based LQR controller and a driver's intention-based fuzzy controller are designed. The weight of the two controllers can be adjusted according to the needs of designers.
2. The co-simulation of MATLAB and Carsim is executed, and the lateral motion controller based on shared control can better track the prescribed trajectory with a permissible deviation.

2. T-FVDM

The driving control of intelligent vehicles mainly includes the longitudinal and lateral control. The longitudinal control means that the vehicles adjust the speed to maintain enough space between vehicles, via uses the least amount of braking to ensures a relatively constant speed. The lateral control refers to path tracking with driving safety and ride comfort, which enables vehicles to follow the desired path through automatic steering control.

When vehicles travel on good roads with a low speed, there is generally no need to consider the stability control and other dynamic problems. Hence the kinematic model-based design of the path tracking controller has a reliable control performance. However, intelligent vehicles sometimes travel at high speed in complex traffic environments, and a more accurate vehicle dynamic model is necessary to design for improving the reliable controller. Accordingly, the lateral dynamic model is the basis of the shared control system [23].

The T-FVDM describes the vehicle dynamic system with some simplifications and assumptions, which simplifies the analysis process and retains the most basic vehicle dynamics. Therefore, it has a wide range of applications in vehicle dynamic research and vehicle control. Although the T-FVDM is simple, it quantifies the key parameters affecting the lateral motion of the vehicle, including the position of the vehicle's center of mass and the lateral deflection characteristics of the tires. Clearly, these are the basis for studying the manipulating stability of vehicles [24]. In this paper, according to the principles of vehicle dynamics, a T-FVDM is established, which takes into account two freedoms of vehicles, i.e., lateral and yaw.

As shown in Figure 1, l_f is the front axle wheelbase, l_r is the rear axle wheelbase, a_f is the vehicle sideslip angle of the front wheel, and a_r is the vehicle sideslip angle of the rear wheel; v_x is the longitudinal speed, and v_y is the lateral speed; ω, φ, δ_f are the yaw velocity, the yaw angle, and the front wheel angle, respectively.
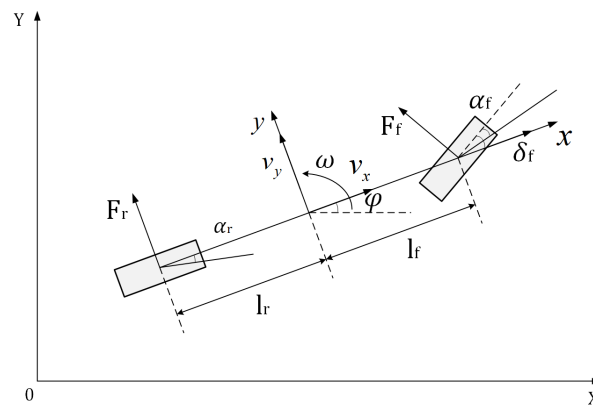
Figure 1. Two-degree of freedom vehicle dynamic model.

When the longitudinal speed of the vehicle is determined, only the motion of the vehicle in both lateral and yaw dimensions are focused, and the lateral forces F_f and F_r on the front and rear wheels can be expressed as:

$$\begin{cases} F_f = C_f \left[\delta_f - \dfrac{(v_y + l_f \varphi)}{v_x} \right] \\ F_r = -\dfrac{C_r (v_y - l_r \varphi)}{v_x}, \end{cases} \tag{1}$$

where C_f is the cornering stiffness of the front tire, and C_r is the cornering stiffness of the rear tire.

The dynamic differential equations of the lateral and yaw motion are

$$\begin{cases} 2F_f \cos\delta_f + 2F_r = m(\dot{v}_y - v_x \dot{\varphi}) \\ 2l_r F_f \cos\delta_f - 2l_f F_r = I\ddot{\varphi}, \end{cases} \tag{2}$$

where m and I are the known mass and rotational inertia with the established vehicle, respectively, and other parameters have been explained thereinbefore. It is noted that the lateral force on the front and rear is twice as much as the lateral force of the corresponding tire.

The conversion between the coordinate system of vehicles and the inertial coordinate system, is

$$\begin{cases} P_X = \dot{p}_x \cos\varphi - \dot{p}_y \sin\varphi, \\ P_Y = \dot{p}_x \sin\varphi - \dot{p}_y \cos\varphi. \end{cases} \tag{3}$$

where P_X and P_Y are the positions in terms of X and Y directions in the global coordinate system, respectively; p_x and p_y are the positions in terms of x and y directions in the vehicle local coordinate system. Furthermore, the linear equation of state is simplified as follows:

$$\begin{pmatrix} \ddot{v}_y \\ \ddot{\varphi} \end{pmatrix} = \begin{pmatrix} \dfrac{C_f + C_r}{m v_x} & \dfrac{l_r C_f - l_f C_r}{m v_x} - v_x \\ \dfrac{l_r C_f - l_f C_r}{I v_x} & \dfrac{l_r^2 C_f + l_f^2 C_r}{I v_x} \end{pmatrix} \begin{pmatrix} \dot{v}_y \\ \dot{\varphi} \end{pmatrix} + \begin{pmatrix} -\dfrac{C_f}{m v_x} \\ -\dfrac{l_r C_f}{I} \end{pmatrix} \delta_f \tag{4}$$

3. Shared Control

Shared control was first proposed by Sheridan and Verplank, and was defined as "a situation where both automation and humans work on the same task at the same time" [25]. It is generally believed that intelligent control systems are good at the execution of fine tasks, while humans are skilled in the judgment and upper-level planning. Moreover,

humans can monitor the operating status of the robotic system in real time and correct some errors. Therefore, in many cases, it is necessary to rely on humans and intelligent control systems to complete complex tasks [22]. For intelligent vehicles, the movement is completely determined by the intelligent control system. However, if a driver intervenes, the movement is determined by the driver. For the existing problem, the human–machine shared control is an acceptable solution, and it can determine the movement behavior of the vehicle together with the driver [19,26–28].

In shared control system of vehicles as shown in Figure 2, a weighting operation is needed to coordinate the control behavior of the driver and the intelligent control system, it is

$$u_{\text{s}} = \lambda u_{\text{a}} + (1 - \lambda)u_{\text{h}},\ 0 \leq \lambda \leq 1, \tag{5}$$

where u_{s} is the shared control input, u_{a} is the control command of the intelligent vehicle autopilot system, u_{h} is the driver's intention-based control input, and λ is the adjustable weight coefficient.
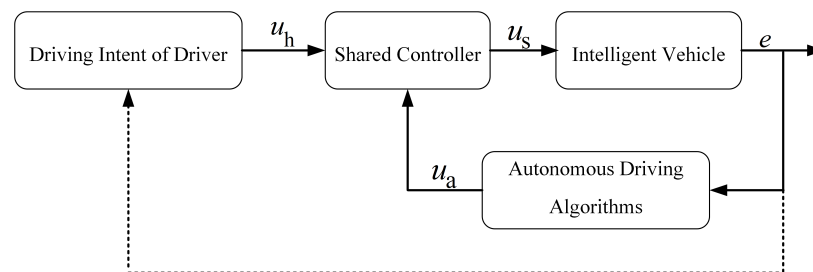

Figure 2. The control framework based on shared control.

Remark 1. *In the proposed shared control scheme, it is assumed that both the intelligent control system and the driver have a perception of the external environment. The autonomous driving system controls the steering angle through the control input of an LQR controller (see Equation (10)). Accordingly, the driver controls the steering angle of the vehicle through a fuzzy controller, which uses fuzzy rules to deduce control commands in the Driver Intent Recognition part.*

4. LQR Algorithm for Intelligent Vehicles

LQR optimal control has the ability to achieve the desired performance index with low cost, and to tune the unstable system simultaneously [29–31]. When the intelligent vehicle tracks the target path, the distance and heading deviations need to be considered. To be clearer, they are described in Figure 3. The distance deviation e_{d} is the distance from the centroid of the vehicle to the road centerline, and the heading deviation e_{φ} is the deviation between the vehicle heading and the road direction; φ_{des} is the ideal heading angle.
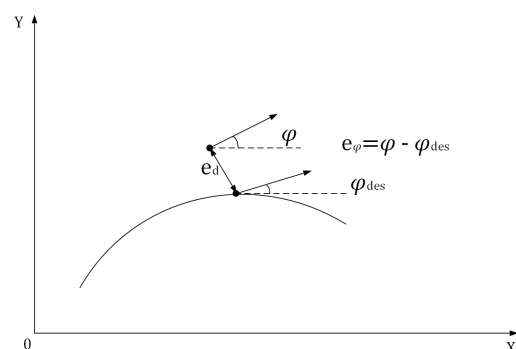

Figure 3. Distance deviation and heading deviation.

For the deviations e_{d} and e_{φ}, the equations are obtained as

$$\ddot{e}_d = -\frac{C_f + C_r}{mv_x}\dot{e}_d + \frac{C_f + C_r}{m}e_\varphi + \frac{l_f\,C_f - l_r\,C_r}{mv_x}\dot{e}_\varphi + \frac{C_f}{m}\delta_f - \left(\frac{l_f C_f - l_r C_r}{mv_x} - v_x\right)\dot{\Psi}_{des}. \quad (6)$$

$$\ddot{e}_\varphi = -\frac{l_f\,C_f - l_r\,C_r}{Iv_x}\dot{e}_d + \frac{l_f\,C_f - l_r\,C_r}{I}e_\varphi - \frac{l_r^{\,2}\,C_r + l_f^{\,2}\,C_f}{Iv_x}\dot{e}_\varphi + \frac{l_f\,C_f}{Iv_x}\delta_f - \left(\frac{l_f^2 C_f - l_r^2 C_r}{Iv_x}\right)\dot{\Psi}_{des}. \quad (7)$$

where $\Psi_{des} = \dfrac{v_x}{R_r}$ is the yaw rate reference, and R_r is the turning radius of the planned path.

Let $x = \begin{bmatrix} e^T_d & \dot{e}^T_d & e^T_\varphi & \dot{e}^T_\varphi \end{bmatrix}^T$, we have

$$\dot{x} = Ax + B_1 u_a + B_2\dot{\Psi}_{des}. \quad (8)$$

where A, B_1 and B_2 represent the state transition matrix, control matrix and feedforward matrix of the continuous-time vehicle model, respectively, and the details are

$$A = \begin{bmatrix} 0 & 1 & 0 & 0 \\ 0 & -\frac{C_f + C_r}{mv_x} & \frac{C_f + C_r}{m} & \frac{-l_f\,C_f + l_r\,C_r}{mv_x} \\ 0 & 0 & 0 & 1 \\ 0 & -\frac{l_f\,C_f - l_r\,C_r}{Iv_x} & \frac{l_f\,C_f - l_r\,C_r}{I} & -\frac{l_f^{\,2}\,C_f + l_f^{\,2}\,C_f}{Iv_x} \end{bmatrix},$$

$$B_1 = \begin{bmatrix} 0 \\ \frac{C_f}{m} \\ 0 \\ \frac{l_f\,C_f}{Iv_x} \end{bmatrix}, \qquad B_2 = \begin{bmatrix} 0 \\ -\frac{l_f C_f - l_r C_r}{mv_x} - v_x \\ 0 \\ -\frac{l_f^2 C_f + l_r^2 C_r}{Iv_x} \end{bmatrix}.$$

Remark 2. *In [32], the yaw rate reference was introduced and used to obtain the corresponding error. Similarly, it has been also used in Equations (6) and (7) (see the terms e_φ and $\dot{e}_\varphi$).*

Using the LQR control theory to design a lateral controller for autonomous driving, the control system performance indicator is

$$J = \int_0^\infty \left[x^T Q x + u_a^T R u_a\right] dt, \quad (9)$$

where Q and R are the positive definite weighting matrixs. The control law of the LQR controller is designed as

$$u_a = -Kx + \delta_{ff} = -R^{-1}B_1^T Px + \delta_{ff}, \quad (10)$$

$$\delta_{ff} = \frac{mv_x^2}{R_r L}\left[\frac{l_r}{2C_f} - \frac{l_f}{2C_r} + \frac{l_f}{2C_r}k_3\right] + \frac{L}{R_r} - \frac{l_r}{R_r}k_3, \quad (11)$$

where $K = [k_1, k_2, k_3, k_4]$, δ_{ff} is the feedforward component of steering angle, $L = (l_f + l_r)$ is the total wheel base, and P is the positive definite solution of the following well-known algebraic Riccati equation:

$$A^T P + PA + Q - PB_1 R^{-1}B_1^T P = 0. \quad (12)$$

5. Driver Intent Recognition

At present, the driver's intent is crucial and has been widely used in intelligent driver assistance systems and autonomous driving systems, such as driving intent for lane changing, steering, starting, parking and braking. Based on the GHMM/GGAP-RBFNN hybrid model, the driver's braking intention recognition model was studied to improve the accuracy of normal braking and light braking in [33]. The prediction of steering intention was given via a novel hybrid algorithm of the time-series model based on deep learning in [34]. In [35], driving intention recognition was extracted and dynamically identified based on the rough set theory and back-propagation artificial neural networks.

Considering the complexity of the lateral control, such as nonlinearity of the driving process and the difficulty of obtaining the accurate model, the fuzzy control method is introduced to transform the driver's input into the control input of intelligent vehicles. The angular deviation e_φ and the angular deviation rate $\dot{e}_\varphi$ are the input variables, and the angle increment u_h of the front wheel is the output variable. $\{NB, NM, NS, ZO, PS, PM, PB\}$ are the fuzzy sets of e_φ, $\dot{e}_\varphi$ and u_h. Both input and output membership functions are taken as triangular membership functions. Based on the summary of skilled drivers' experience and control engineering knowledge, 49 rules were formulated in Table 1. According to the designed fuzzy rules, the fuzzy output is obtained by fuzzy inference with the driver's input. Next, the centroid method is used for defuzzification, and the control input of the front wheel angle is obtained.

Table 1. Fuzzy control rules.

u_h		$\dot{e}_\varphi$						
		NB	NM	NS	ZO	PS	PM	PB
	NB	NB	NB	NM	NM	NS	NS	ZO
	NM	NB	NM	NM	NS	NS	ZO	PS
e_φ	NS	NM	NM	NS	NS	ZO	PS	PS
	ZO	NM	NS	NS	ZO	PS	PS	PM
	PS	NS	NS	ZO	PS	PS	PM	PM
	PM	NS	ZO	PS	PS	PM	PM	PB
	PB	ZO	PS	PS	PM	PM	PB	PB

6. Simulation Results

In order to verify the proposed control scheme, a Co-Simulation of CarSim and MATLAB is performed in this section. CarSim is a simulation software for vehicle dynamics, which can simulate the response of a vehicle to the road and aerodynamic inputs. It is mainly used to predict and simulate the handling stability, braking, smoothness, power and economy of the whole vehicle [33].

In CarSim, the C-class passenger car model is adopted, and the main parameters are shown in Table 2. The fixed vehicle speed is controlled by the controller in Carsim, and the front-wheel turning angle is calculated by the controller in the Simulink.

In Figure 4, the shared control is achieved by combining the driver's intention-based fuzzy control algorithm and the LQR-based automatic driving algorithm.

The simulation results are shown in Figures 5 and 6. It can be seen that the LQR and shared controllers can track the planned path well, as shown in in Figure 5. For a comparison, the distance deviations of LQR and shared controllers are given in Figure 6, The tracking performance of the lateral controller based on shared control is better than that of the LQR-based autonomous driving controller. To quantify the results of the LQR control and the shared control, we introduce e_{Lx} and e_{Ly}, which are the trajectory tracking errors of

the LQR control in terms of x and y directions, respectively. Accordingly, e_{Sx} and e_{Sy} are the trajectory tracking errors of the share control in terms of x and y directions, respectively. For comparison, the performance index $E = \sum_{t=0}^{30}(\|e_{.x}\|_1 + \|e_{.y}\|_1)$ is calculated for the LQR control and shared control cases, respectively, i.e., 3.8395×10^6 and 3.8198×10^6. Clearly, the superiority of the proposed shared control method is verified.

Table 2. Main parameters of the vehicle.

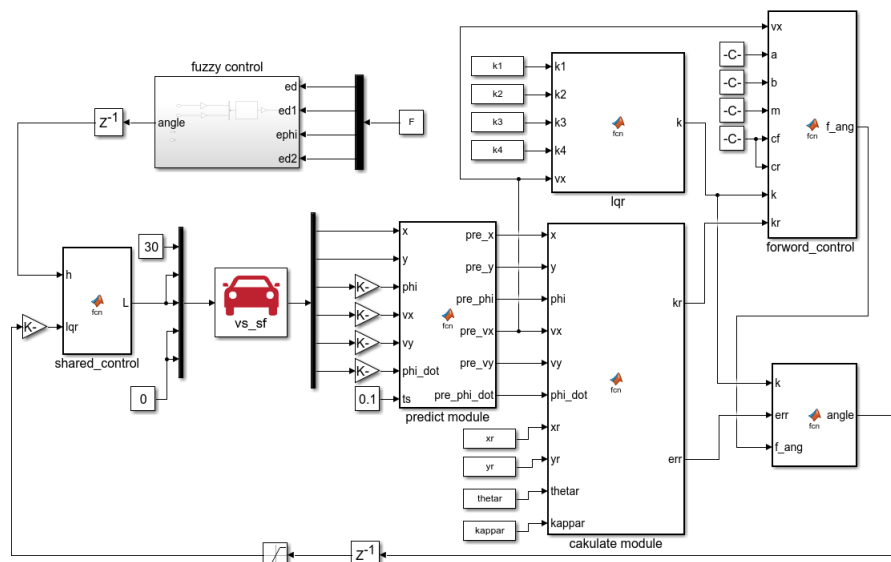| Name (Unit)	Symbol	Numerical
vehicle quality (kg)	m	1412
moment of inertia of the vehicle (kg·m^2)	I	1536.7
cornering stiffness of the front wheel (N/rad)	C_f	−110,000
cornering stiffness of the rear wheel (N/rad)	C_r	−110,000
front wheelbase (m)	l_f	1.015
rear wheelbase (m)	l_r	1.895

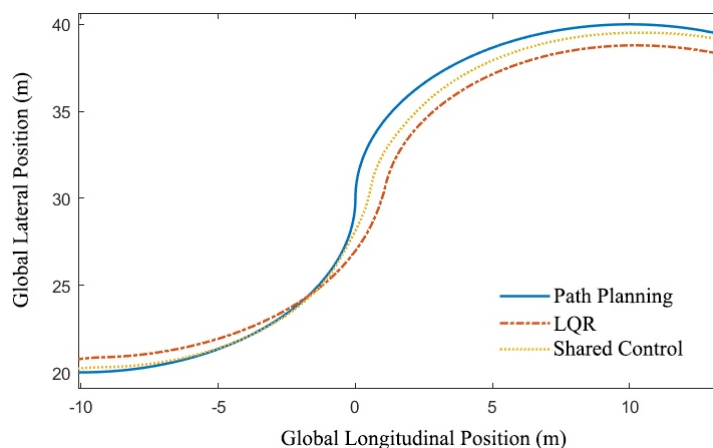**Figure 4.** Matlab/Carsim simulation model.

Figure 5. The portion of tracking trajectory of LQR control and the shared control.
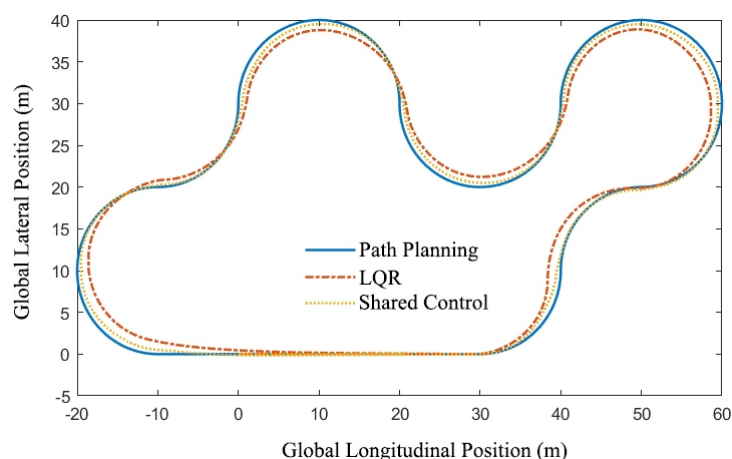
Figure 6. Tracking trajectory of LQR control and the shared control.

7. Conclusions

For the intelligent vehicle control system with the driver's participation, this paper proposed a control scheme for the lateral motion based on shared control. With the constructed T-FVDM, an LQR controller for autonomous driving system and a fuzzy control-based controller have been designed. Based on these controllers, the lateral controller hwas constructed according to the shared control method. Through the co-simulation of MATLAB/Simulink and Carsim, the simulation results showed that the lateral controller based on shared control has provided better tracking performance than the LQR-based controller. In our future work, the shared control of intelligent vehicles using data-driven techniques will be further investigated [36–38], even considering non-cooperative behaviors [39–44].

Author Contributions: Conceptualization, G.L.; methodology, G.L. and D.S.; validation, G.L. and P.S.; investigation, G.L. and P.S.; writing—original draft preparation, G.L., P.S. and C.Z.; writing—review and editing, G.L., P.S. and C.Z.; visualization, G.L., P.S. and C.Z.; supervision, D.S.; funding acquisition, G.L. and D.S. All authors have read and agreed to the published version of the manuscript.

Institutional Review Board Statement: Not applicable.

Informed Consent Statement: Not applicable.

Data Availability Statement: Not applicable.

Conflicts of Interest: The authors declare no conflict of interest.

Abbreviations

For the convenience of readers, all the symbols involved in the paper are summarized and listed in the table.

Symbol	Name	Units
l_f	front axle wheelbase	m
l_r	rear axle wheelbase	m
L	total wheel base	m
a_f	vehicle sideslip angle of the front wheel	deg
a_r	vehicle sideslip angle of the rear wheel	deg
v_x	longitudinal speed	km/h
v_y	lateral speed	km/h
ω	yaw velocity	rad/s
φ	yaw angle	deg
δ_f	front wheel angle	deg
δ_{ff}	feedforward component of steering angle	deg

C_f	cornering stiffness of the front wheel	N/rad
C_r	cornering stiffness of the rear wheel	N/rad
m	vehicle quality	kg
I	moment of inertia of the vehicle	kg·m^2
R_r	turning radius of the planned path	m
Ψ_des	yaw rate reference	
u_s	shared control input	
u_a	control command of the vehicle autopilot system	
u_h	driver's control intention-based control input	
λ	adjustable weight coefficient	

References

1. Zhang, Z.Y.; Wang, X.J.; Huang, D.; Fang, X.; Zhou, M.; Zhang, Y. MPPT: Millimeter-wave radar-based pedestrian trajectory tracking for autonomous urban driving. *IEEE Trans. Instrum. Meas.* **2022**, *71*, 1–17.
2. Zheng, C.-B.; Pang, Z.-H.; Wang, J.X.; Sun, J.; Liu, G.-P.; Han, Q.-L. Null-space-based time-varying formation control of uncertain nonlinear second-order multi-agent systems with collision avoidance. *IEEE Trans. Ind. Electron.* **2022**, 1–10. [CrossRef]
3. Huang, D.; Zhou, J.F.; Mi, B.; Kuang, F.T.; Liu, Y. Key-based data deduplication via homomorphic NTRU for internet of vehicles. *IEEE Trans. Veh. Technol.* **2022**, 1–14. [CrossRef]
4. Pang, Z.-H.; Zheng, C.-B.; Li, C.; Liu, G.-P.; Han, Q.-L. Cloud-based time-varying formation predictive control of multi-agent systems with random communication constraints and quantized signals. *IEEE Trans. Circuits Syst. II Express Briefs* **2022**, *69*, 1282–1286. [CrossRef]
5. Ahmad, E.; Iqbal, J.; Arshad, K.M.; Liang, W.; Youn, I. Predictive control using active aerodynamic surfaces to improve ride quality of a vehicle. *Electronics* **2020**, *9*, 1463. [CrossRef]
6. Hu, L.; Zhou, X.; Zhang, X. A review on key challenges in intelligent vehicles: Safety and driver-oriented features. *IET Intel. Transport Syst.* **2021**, *15*, 1093–1105. [CrossRef]
7. Guanetti, J.; Kim, Y.J.; Borrelli, F. Control of connected and automated vehicles: State of the art and future challenges. *Annu. Rev. Control* **2018**, *45*, 18–40. [CrossRef]
8. Pang, Z.-H.; Luo, W.-C.; Liu, G.-P.; Han, Q.-L. Observer-based incremental predictive control of networked multi-agent systems with random delays and packet dropouts. *IEEE Trans. Circuits Syst. II Express Briefs* **2021**, *68*, 426–430. [CrossRef]
9. Pang, Z.; Bai, C.; Liu, G.; Han, Q.; Zhang, X. A novel networked predictive control method for systems with random communication constraints. *J. Syst. Sci. Complex.* **2021**, *34*, 1364–1378. [CrossRef]
10. Badue, C.; Guidolini, R.; Carneiro, R.V. Self-driving cars: A survey. *Expert Syst. Appl.* **2020**, 165, 113816. [CrossRef]
11. Wiseman, Y. COVID-19 Along with autonomous vehicles will put an end to rail systems in isolated territories. *IEEE Intell. Transp. Syst. Mag.* **2021**, 13, 6–12. [CrossRef]
12. Elias, J. Waymo Says It Plans to Launch Its Self-Driving Service in Los Angeles. Available online: https://www.cnbc.com/2022/10/19/waymo-says-it-plans-to-launch-a-ride-hailing-service-in-los-angeles.html (accessed on 19 October 2022).
13. Jiang, Y.; Zhang, X.; Xu, X; Zhou, X.; Dong, Z. Event-triggered shared lateral control for safe-maneuver of intelligent vehicles. *Sci. China Inf. Sci.* **2021**, *64*, 172203. [CrossRef]
14. Bustamante, S.; Quere, G.; Hagmann, K. Toward seamless transitions between shared control and supervised autonomy in robotic assistance. *IEEE Rob. Autom. Lett.* **2021**, *6*, 3833–3840. [CrossRef]
15. Zhang, B.; Holloway, C.; Carlson, T. A hierarchical design for shared-control wheelchair navigation in dynamic environments. In Proceedings of the 2020 IEEE International Conference on Systems, Man, and Cybernetics (SMC), Toronto, ON, Canada, 11–14 October 2020; pp. 4439–4446.
16. Quere, G.; Bustamante, S.; Hagengruber, A. Learning and interactive design of shared control templates. In Proceedings of the 2021 IEEE/RSJ International Conference on Intelligent Robots and Systems (IROS), Prague, Czech Republic, 27 September–1 October 2021; pp. 1887–1894
17. Dwivedi, A.; Shieff, D.; Turner, A. A shared control framework for robotic telemanipulation combining electromyography based motion estimation and compliance control. In Proceedings of the IEEE International Conference on Robotics and Automation (ICRA), Xi'an, China, 30 May–5 June 2021; pp. 9467–9473.
18. Abbink, D.A.; Carlson, T.; Mulder, M.; De Winter; J.C.; Aminravan, F.; Gibo, T.L.; Boer, E.R. A topology of shared control systems—Finding common ground in diversity. *IEEE Trans. Hum.-Mach. Syst.* **2018**, *48*, 509–525. [CrossRef]
19. Marcano, M.; Díaz, S.; Pérez, J.; Irigoyen, E. A review of shared control for automated vehicles: Theory and applications. *IEEE Trans. Hum.-Mach. Syst.* **2020**, *50*, 475–491. [CrossRef]
20. Marcano, M.; Castellano, A.; Díaz, S.; Pérez, J.; Tango, F.; Landini, E.; Burgio, P. Shared and traded control for human-automation interaction: A haptic steering controller and a visual interface. *Springer Ser. Hurm.-Intell. Syst. Integr.* **2021**, *3*, 25–35. [CrossRef]
21. Li, M.; Cao, H.; Song, X.; Huang, Y.; Wang, J.; Huang, Z. Shared control driver assistance system based on driving intention and situation assessment. *IEEE Trans. Ind. Inf.* **2018**, *14*, 4982–4994. [CrossRef]
22. Wang, W.; Na, X.; Cao, D.; Gong, J.; Xi, J.; Xing, Y.; Wang, F.Y. Decision-making in driver-automation shared control: A review and perspectives. *IEEE/CAA J. Autom. Sin.* **2020**, *7*, 1289–1307. [CrossRef]

23. Khan, H.; Iqbal, J.; Baizid, K.; Zielinska, T. Longitudinal and lateral slip control of autonomous wheeled mobile robot for trajectory tracking. *Front. Inf. Technol. Electron. Eng.* **2015**, *16*, 166–172. [CrossRef]
24. Zhang, L. B.; Zhou, Z.; Ma, Y.; Zhang, S. Co-simulation study of automobile two-degree-of-freedom steering model and VTD scenario model. In Proceedings of the 2021 IEEE 2nd International Conference on Information Technology, Big Data and Artificial Intelligence (ICIBA), Chongqing, China, 17–19 December 2021; pp. 365–369.
25. Sheridan, T.B.; Verplank, W.L.; Brooks, T.L. Human and computer control of undersea teleoperators. *Hum. Comput. Control Undersea Telop.* **1978**.
26. Fang, H.; Shang, C.S.; Chen, J. An optimization-based shared control framework with applications in multi-robot systems. *Sci. China Inf. Sci.* **2018**, *61*, 261–263. [CrossRef]
27. Xing, Y.; Huang, C.; Lv, C. Driver-automation collaboration for automated vehicles: A review of human-centered shared control. In Proceedings of the 2020 IEEE Intelligent Vehicles Symposium (IV), Las Vegas, NV, USA, 19 October–13 November 2020; pp. 1964–1971.
28. Chouki, S.; Anh-Tu, N.; Amir, B.M. Driver-automation cooperation oriented approach for shared control of lane keeping assist systems. *IEEE Trans. Control Syst. Technol.* **2019**, *27*, 1962–1978.
29. Yang, T.; Bai, Z.; Li, Z.; Feng, N.; Chen, L. Intelligent vehicles lateral control method based on feedforward + predictive LQR algorithm. *Actuators* **2021**, *10*, 228. [CrossRef]
30. Pang, Z.-H.; Liu, G.-P.; Zhou, D.; Hou, F.; Sun, D. Two-channel false data injection attacks against output tracking control of networked systems. *IEEE Trans. Ind. Electron.* **2016**, *63*, 3242–3251. [CrossRef]
31. Asghar, A.; Iqbal, M.; Khaliq, A.; Rehman, S.U.; Iqbal, J. Performance comparison of structured H_∞ based looptune and LQR for a 4-DOF robotic manipulator. *PLoS ONE* **2022**, *17*, e0266728. [CrossRef]
32. Rajamani, R. *Vehicle Dynamics and Control*; Springer Science & Business Media: Berlin, Germany, 2011.
33. Zhao, X.; Wang, S.; Ma, J.; Yu, Q.; Gao, Q.; Yu, M. Identification of driver's braking intention based on a hybrid model of GHMM and GGAP-RBFNN. *Springer Ser. Neural Comput. Appl.* **2019**, *31*, 161–174. [CrossRef]
34. Xing, Y.; Lv, C.; Liu, Y.; Zhao, Y.; Cao, D.; Kawahara, S. Hybrid-learningbBased driver steering intention prediction using neuromuscular dynamics. *IEEE Trans. Ind. Electron.* **2020**, *69*, 1750–1761. [CrossRef]
35. Wang, X.Y.; Liu, Y.Q.; Xu, Q.; Xia, Y.Y.; Zhao, H.X.; Liu, S. J.; Han, J.Y. Feature extraction and dynamic identification of driving intention adapting to multi-mode emotions. *Adv. Mech. Eng.* **2019**, *11*, 1–14. [CrossRef]
36. Pang, Z.-H.; Zhao, X.-Y.; Sun, J.; Shi, Y.; Liu, G.-P. Comparison of three data-driven networked predictive control methods for a class of nonlinear systems. *IEEE/CAA J. Autom. Sin.* **2022**, *9*, 1714–1716. [CrossRef]
37. Pang, Z.-H.; Ma, B.; Liu, G.-P; Han, Q.-L. Data-driven adaptive control: An incremental triangular dynamic linearization approach. *IEEE Trans. Circuits Syst. II Express Briefs* **2022**. [CrossRef]
38. Guo, W.; Cao, H.; Zhao, S.; Li, M.; Yi, B.; Song, X. A data-driven model-based shared control strategy considering drivers' adaptive behavior in driver-automation interaction. *Proc. Inst. Mech. Eng. Part D J. Automob. Eng.* **2022**. [CrossRef]
39. Jugade, S.C.; Victorino, A.C.; Cherfaoui, V.B. Shared driving control between human and autonomous driving system via conflict resolution using non-cooperative game theory. In Proceedings of the 2019 IEEE Intelligent Transportation Systems Conference (ITSC), Auckland, New Zealand, 27–30 October 2019; pp. 2141–2147.
40. Pang, Z.-H.; Fan, L.-Z.; Sun, J.; Liu, K.; Liu, G.-P. Detection of stealthy false data injection attacks against networked control systems via active data modification. *Inf. Sci.* **2021**, *546*, 192–205. [CrossRef]
41. Pang, Z.-H.; Fan, L.-Z.; Dong, Z.; Han, Q.-L.; Liu, G.-P. False data injection attacks against partial sensor measurements of networked control systems. *IEEE Trans. Circuits Syst. II Express Briefs* **2022**, *69*, 149–153. [CrossRef]
42. Pang, Z.; Fu, Y.; Guo, H.; Sun, J. Analysis of stealthy false data injection attacks against networked control systems: Three case studies. *J. Syst. Sci. Complex.* **2022**. [CrossRef]
43. Pang, Z.-H.; Fan, L.-Z.; Guo, H.; Shi, Y.; Chai, R.; Sun, J.; Liu, G.-P. Security of networked control systems subject to deception attacks: A survey. *Int. J. Syst. Sci.* **2022**. [CrossRef]
44. Liu, J.; Dai, Q.; Guo, H.; Guo, J.; Chen, H. Human-oriented online driving authority optimization for driver-automation shared steering control. *IEEE Trans. Intell. Veh.* **2022**. [CrossRef]